Nuclear Engineering and Technology 48 (2016) 339–350

Available online at ScienceDirect

Nuclear Engineering and Technology

journal homepage: www.elsevier.com/locate/net

Original Article

# Resonance Elastic Scattering and Interference Effects Treatments in Subgroup Method

*Yunzhao Li*[*], *Qingming He, Liangzhi Cao, Hongchun Wu, and Tiejun Zu*

*School of Nuclear Science and Technology, Xi'an Jiaotong University, 28 West Xianning Road, Xi'an, Shaanxi 710049, China*

ARTICLE INFO

*Article history:*
Received 25 November 2015
Received in revised form
28 December 2015
Accepted 30 December 2015
Available online 3 March 2016

*Keywords:*
Doppler Broadening Rejection Correction
Fast Resonance Interference Factor
Resonance Elastic Scattering Effect
Resonance Interference Effect
Subgroup Method

ABSTRACT

Based on the resonance integral (RI) tables produced by the NJOY program, the conventional subgroup method usually ignores both the resonance elastic scattering and the resonance interference effects. In this paper, on one hand, to correct the resonance elastic scattering effect, RI tables are regenerated by using the Monte Carlo code, OpenMC, which employs the Doppler broadening rejection correction method for the resonance elastic scattering. On the other hand, a fast resonance interference factor method is proposed to efficiently handle the resonance interference effect. Encouraging conclusions have been indicated by the numerical results. (1) For a hot full power pressurized water reactor fuel pin-cell, an error of about +200 percent mille could be introduced by neglecting the resonance elastic scattering effect. By contrast, the approach employed in this paper can eliminate the error. (2) The fast resonance interference factor method possesses higher precision and higher efficiency than the conventional Bondarenko iteration method. Correspondingly, if the fast resonance interference factor method proposed in this paper is employed, the $k_{inf}$ can be improved by ~100 percent mille with a speedup of about 4.56.


## 1. Introduction

The subgroup method [1,2] is widely employed by nuclear reactor neutronic codes such as DeCART [3,4] and MPACT [5] for its geometrical flexibility and high accuracy compared to the conventional equivalence theory. There are two main steps in the subgroup method: (1) probability tables are obtained from the resonance integral (RI) tables [6]; and (2) subgroup fixed source problems are solved by using mature multigroup transport solvers. The RI tables are typically obtained by solving a series of slowing down problems over a range of background cross sections using the hyperfine energy group method or the Monte Carlo (MC) method. In fact, this introduces two approximations by ignoring the resonance elastic scattering and interference effects.

* *Corresponding author.*
E-mail address: yunzhao@mail.xjtu.edu.cn (Y. Li).
http://dx.doi.org/10.1016/j.net.2015.12.015

In the hyperfine energy group method, the asymptotic scattering kernel is usually employed to obtain the scattering source. The asymptotic scattering kernel ignores the up-scattering of neutrons in the epithermal energy range [7]. In the MC method, the elastic scattering cross sections are assumed to be constant at 0 K in the free gas model, which is invalid for heavy nuclides with large resonance peaks [8]. As a consequence, multiplication factors would be over-estimated, which is the so-called resonance elastic scattering [9–11] or neutron up-scattering effect [12–14]. In a stochastic method, Rothenstein [15], Dagan [16], and Becker et al. [17] used the $S(\alpha,\beta)$ table that stores cross sections for different energies and scattering angles to take this effect into account. However, the $S(\alpha,\beta)$ table can only be prepared at several temperatures and may introduce many errors in performing temperature interpolation. Therefore, a stochastic method named the Doppler broadening rejection correction (DBRC) method was proposed [11,17]. It samples the target velocity on-the-fly to instead of preparing $S(\alpha,\beta)$ table for specified temperatures. It is more accurate and stable but consumes more computing time than the $S(\alpha,\beta)$ method. Lee et al. [9] and Mori and Nagoya [18] developed the weight correction method (WCM) to save computation time. Unfortunately, its disadvantage is the increase of variance due to the fact that the weight correction factor may deviate significantly from unity [18]. By contrast, to consider this effect in deterministic codes, Lee et al. [9] solved the neutron slowing down problems to generate the RI tables by developing an MC code with an exact scattering kernel, while Lim et al. [12] implemented the Doppler broadening rejection correction (DBRC) into the McCARD code [19] to generate cross sections for the nTRACER [4] code. In this paper, to introduce the Doppler broadened scattering kernel into the multigroup deterministic method, the MC code OpenMC [20] is modified via DBRC and used to generate resonance elastic correction factor tables.

Only one resonant nuclide and one nonresonant are contained in the infinite homogeneous problems for which the neutron slowing down equation is solved to produce the RI tables. In this case, the interference between the resonance peaks of different nuclides cannot be taken into account. It leads to the so-called resonance interference effect. The Bondarenko iteration method [21] was conventionally employed to correct this effect. In this method, when performing resonance calculations of one resonant nuclide, all other resonant nuclides are considered to be background nuclides with constant cross sections. An iteration between different resonant nuclides was carried out to converge the background and self-shielded cross sections. However, it usually consumes too much computing time. Consequently, there are two classes of method developed to improve the resonance interference treatment.

The first class treated the overlapped energy ranges of different subgroups of different resonant nuclides as new subgroups. In order to determine the overlap energy range, Takeda and Kaneyama [22] suggested figuring out the detailed subgroup energy domain from the continuous total cross section function in terms of energy. A parameter was introduced to define a new subgroup where one nuclide takes a certain subgroup under a given condition while the others take another subgroup. In this new subgroup, the macroscopic subgroup cross sections can be calculated from the subgroup cross sections of the resonant nuclides in their particular subgroups. Therefore the resonance interference effect can be taken into account by solving the subgroup fixed source problem defined in the new subgroups. By contrast, Huang et al. [23] simplified the procedure by assuming that the overlap energy range of different nuclides is stochastic. The parameter is calculated by multiplying the subgroup probability of the corresponding subgroups of different nuclides. Hébert [24] used a two-nuclide correlated matrix to present the overlap energy ranges. These methods show higher precision than the Bondarenko iteration, but, due to their time consumption, are still not applicable to cases with more than two resonant nuclides.

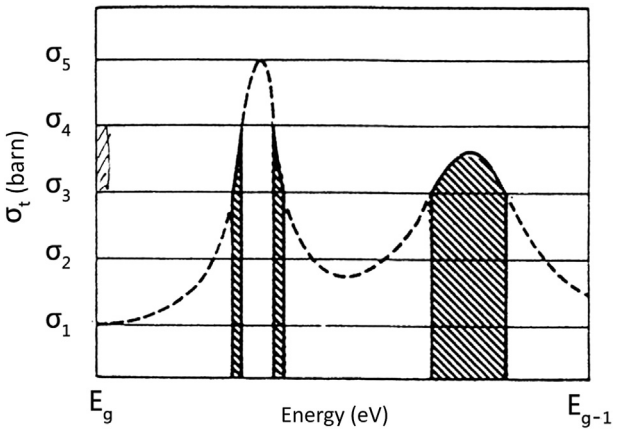


**Fig. 1 – Definition of subgroup according to magnitude of total cross section.**

The other class is the resonance interference factor (RIF) method proposed by Williams [25]. The RIF is the quotient of self-shielded cross sections. The numerator is calculated by considering the entire mixture of all the resonant nuclides, while the denominator is calculated with only one resonant nuclide. These self-shielded cross sections are computed by the hyperfine energy group method or the MC method. The RIF is applied to a self-shielded cross section, calculated by methods such as the subgroup method or equivalence theory, with the assumption that there is only one resonant nuclide in the medium. The RIF can be calculated in either homogeneous or heterogeneous system sinc. Chiba [26] and Kim [27] proved the consistency of these methods. The homogeneous RIF method saves a lot of time compared with the heterogeneous method. If the RIF is calculated on-the-fly, it still consumes too much time. Kim and Hong [28] and Peng et al. [29] tried to prepare the RIF *in-priori* as a function of temperature, dilution cross section, and the ratio of number density. To reduce the storage of the RIF table, the resonance interference effect is assumed to be introduced by the resonant nuclides one after another, rather than simultaneously. The tabulation approach is cheap in computational time but unfortunately may introduce a lot of error for cases with more than two resonant nuclides, such as mixed oxide (MOX) fuel problems. Despite its drawbacks, the RIF method has achieved wide application due to its simplicity. The RIF method and its variants has been

applied to codes such as WIMS [30], LANCER02 [31], MPACT [32], DeCART [33], SCALE [27], STREAM [34], and APOLLO3 [35].

To overcome the drawbacks of the conventional RIF methods, this paper proposes a new method named fast RIF to treat the resonance interference effect.

The rest of this paper is organized as follows. Section 2 briefly introduces the theory of the subgroup method and explains how the resonance elastic scattering and interference effects are corrected to improve the subgroup method. Numerical results in Section 3 demonstrate the improvements. Finally, conclusions and discussions are given in Section 4.

## 2. Theory

### 2.1. Subgroup method

Subgroups are defined according to the magnitude of the total cross sections, as shown in Fig. 1. Taking the third subgroup in group $g$ as an example, the energy domain is:

$$\Delta E_{g,3} \in \{E|\sigma_3 < \sigma(E) \le \sigma_4\} \tag{1}$$

The neutron slowing down equation in a heterogeneous system is:

$$\Omega\nabla\phi(r,u,\Omega) + \sum_t(r,u)\phi(r,u,\Omega) = \frac{1}{4\pi}\int du' \sum_{s0}(r,u'\to u)\phi(r,u') \tag{2}$$

where $u$ is the lethargy, $\sum_t(r,u)$ is the total cross section, and $\sum_{s0}(r,u'\to u)$ is the $0^{th}$ Legendre moment of the scattering cross section [36]. In Eq. (2), the fission source has been ignored considering the fact that almost all fission neutrons are fast ones. By assuming that the scattering is elastic and isotropic in a center-of-mass system and applying narrow resonance approximation, the scattering source can be simplified into:

$$\frac{1}{4\pi}\int d\mu' \sum_{s0}(r,u'\to u)\phi(r,u') = \frac{1}{4\pi}\sum_p(r) \tag{3}$$

where $\sum_p(r)$ is the macroscopic potential scattering cross section.

Integrating the neutron slowing down equation over a subgroup yields the subgroup fixed source problem:

$$\Omega\nabla\phi_{g,i}(r,\Omega) + \sum_{t,g,i}(r)\phi_{g,i}(r,\Omega) = \Delta u_{g,i}\frac{1}{4\pi}\sum_p(r) \tag{4}$$

where $\sum_{t,g,i}(r)$ is the macroscopic subgroup total cross section, $\phi_{g,i}(r,\Omega)$ is the subgroup flux, $\Delta u_{g,i} = p_{g,i}\Delta u_g$ is lethargy width of subgroup i, $p_{g,i}$ is the subgroup probability, and $\Delta u_g$ is the lethargy width of energy group $g$. The subgroup total cross section is defined by:

$$\sum_{t,g,i}(r) = \sum_k N_k(r)\sigma_{t,k,g,i} = \sum_k N_k(r)\frac{\int_{\Delta u_{g,i}}\sigma_{t,k}(u)\phi(u)du}{\int_{\Delta u_{g,i}}\phi(u)du} \tag{5}$$

where $k$ is the nuclide index, $N_k(r)$ is the atom density, $\sigma_{t,k,g,i}$ is the microscopic subgroup total cross section, $\sigma_{t,k}(u)$ is the continuous energy total cross section of nuclide $k$, and $\phi(u)$ is the flux spectrum.

The combination of subgroup cross section and subgroup probability constitutes the subgroup probability table. To obtain this table, an RI table needs to be constructed by using the self-shielded cross section:

$$R_{x,k,g,j} = \sigma_{x,k,g,j}\frac{\sigma_{p,k}+\sigma_{0,j}}{\sigma_{t,k,g,j}+\sigma_{0,j}} \tag{6}$$

where $\sigma_{p,k}$ stands for the microscopic potential scattering cross section of nuclide $k$, and $\sigma_{0,j}$ is $j^{th}$ dilution cross section. The self-shielded cross sections are obtained by solving the neutron slowing down equations over a range of background cross sections. Then a fitting between the resonance integral $R_{t,k,g,j}$ and the dilution cross section $\sigma_{0,j}$ is implemented by minimizing:

$$F\left(\sigma_{t,k,g,1},\cdots,\sigma_{t,k,g,I},p_{k,g,1},\cdots,p_{k,g,I}\right) = \sum_{j=1}^{J}\left[R_{t,k,g,j} - \sum_{i=1}^{I}\frac{\sigma_{t,k,g,i}p_{k,g,i}(\sigma_{p,k}+\sigma_{0,j})}{\sigma_{t,k,g,i}+\sigma_{0,j}}\right]^2 \tag{7}$$

where the subgroup total cross section and subgroup probability are the corresponding fitting coefficients, $I$ is the number of subgroups in Group $g$, and $J$ is the number of dilution cross sections. Other subgroup cross sections can be obtained by minimizing:

$$F\left(\sigma_{x,k,g,1},\cdots,\sigma_{x,k,g,I}\right) = \sum_{j=1}^{J}\left[R_{x,k,g,j} - \sum_{i=1}^{I}\frac{\sigma_{x,k,g,i}p_{k,g,i}(\sigma_{p,k}+\sigma_{0,j})}{\sigma_{t,k,g,i}+\sigma_{0,j}}\right]^2 \tag{8}$$

After obtaining the probability table, Eq. (4) can be solved by using a multigroup transport solver. In this paper, a multigroup transport solver MMOC [37] was employed. After obtaining the subgroup flux, the effective self-shielding cross sections of nuclide $k$ can be obtained:

$$\sigma^{eff}_{x,k,g}(r) = \frac{\int_{4\pi}\sum_i\sigma_{x,k,g,i}(r)\phi_{g,i}(r,\Omega)d\Omega}{\int_{4\pi}\sum_i\phi_{g,i}(r,\Omega)d\Omega} \tag{9}$$

### 2.2. The resonance elastic scattering effect correction

#### 2.2.1. The asymptotic scattering kernel

The neutron slowing down equation of a homogeneous system can be written as:

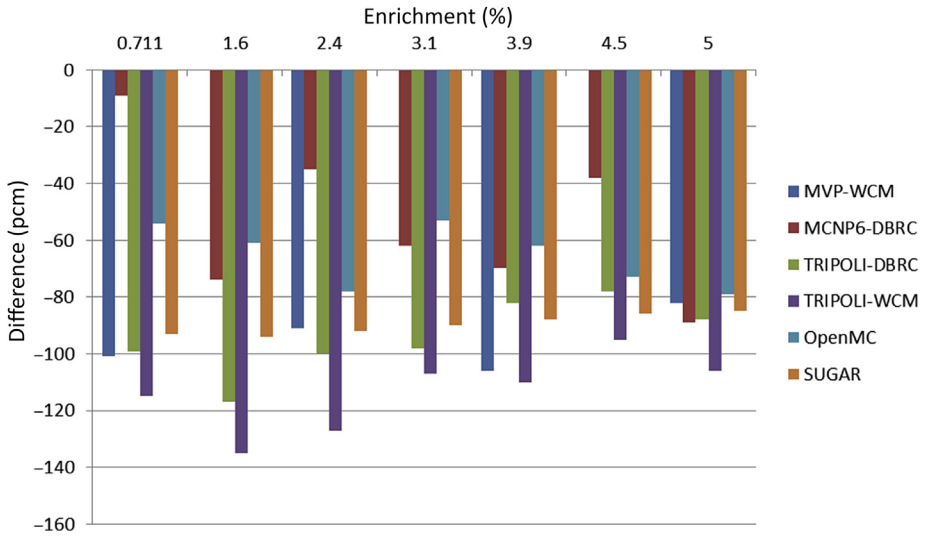


**Fig. 2 – Impact of resonance elastic scattering on $k_\infty$ for $UO_2$ pin cell problems at hot zero power of Mosteller benchmark. PCM, percent mille.**

$$\sum_k \sum_{t,k}(E)\phi(E) = \sum_k \int_0^\infty \sum_{s,k}(E) f_k(E' \to E)\phi(E')dE' \tag{10}$$

where $k$ is nuclide index and $f_k$ is the elastic scattering kernel.

In cross section generation code NJOY [7], or other codes based on the hyperfine energy group method [38–40], the target nuclide is assumed to be at rest. The elastic scattering kernel can then be written as:

$$f_k(E' \to E) = \frac{1}{(1-\alpha_K)E'} \tag{11}$$

where $\alpha_k = (A_k - 1)^2/(A_k + 1)^2$ and $A_k$ is the mass ratio of the target nuclide to the neutron.

Eq. (11) is the asymptotic scattering kernel, which ignores neutron up-scattering.

### 2.2.2. *The conventional free gas model*

The MC method usually employs the free gas model to consider the thermal agitation of the target at elastic collision [8]. Once the velocity of the target is sampled, the velocity of the out-coming neutron can be determined. The probability density function of the target velocity is:

$$P(V, \mu|v_n) = \frac{\sigma_s(v_r, 0)v_r P(V)}{2\sigma_s^{eff}(v_n, T)v_n} \tag{12}$$

where $V$ is the speed of the target, $\mu$ is the cosine of the azimuth angle, $v_n$ is the speed of the neutron, $v_r$ is the relative speed, $T$ is temperature, $P(V)$ is the Maxwell–Boltzmann

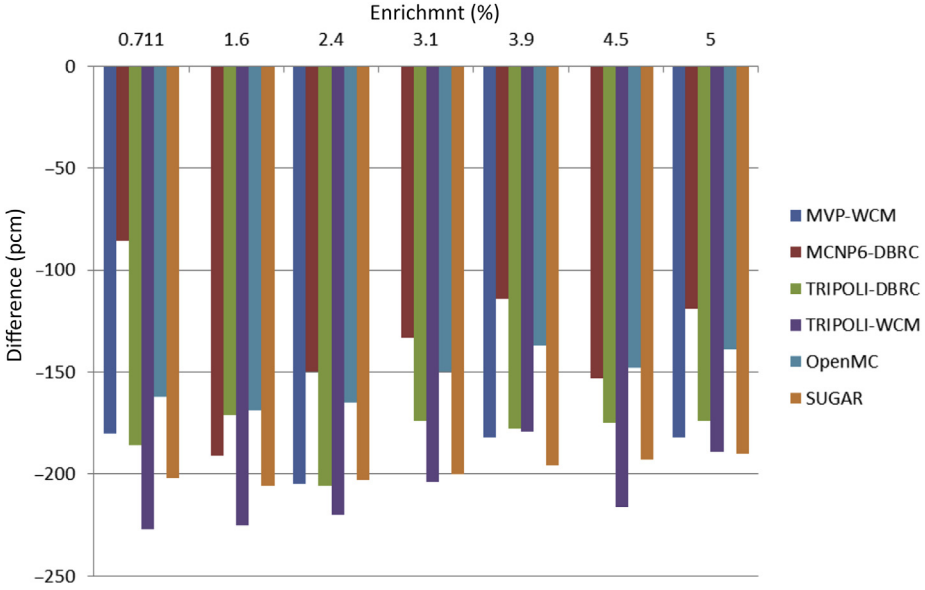


**Fig. 3 – Impact of resonance elastic scattering on $k_\infty$ for $UO_2$ pin cell problems at hot full power of Mosteller benchmark. PCM, percent mille.**

**Table 1 – The resonance severity (RS) of different resonant nuclides for the 80th energy group.**

| Nuclide | Density (atom/b-cm) | RS |
|---|---|---|
| $^{238}$U | 2.1061e-2 | 3.9747e-1 |
| $^{239}$Pu | 8.2425e-4 | 2.1075e-3 |
| $^{240}$Pu | 5.4950e-4 | 1.3404e-3 |
| $^{241}$Pu | 2.7475e-4 | 2.8449e-4 |
| $^{235}$U | 1.5275e-4 | 2.7327e-4 |
| $^{242}$Pu | 1.8317e-4 | 2.0350e-4 |

distribution, $\sigma_s(v_r,0)$ is the elastic scattering cross section at relative speed at zero temperature, and $\sigma_s^{\mathrm{eff}}(v_n,T)$ is the effective elastic scattering cross section.

Assuming that $\sigma_s(v_r,0)$ does not fluctuate with energy, Eq. (12) can be written as:

$$P(V,\mu|v_n) = C\left\{\frac{v_r}{v_n+V}\right\}\{P_1 f_1(V) + P_2 f_2(V)\} \tag{13}$$

where:

$$C = \frac{(2+\sqrt{\pi}\beta v_n)\sigma_s(v_r,0)}{2\sigma_s^{\mathrm{eff}}(v_n,T)\sqrt{\pi}\beta v_n} \tag{14}$$

$$P_1 = \frac{1}{1+\frac{\sqrt{\pi}\beta v_n}{2}} \tag{15}$$

$$P_2 = 1 - P_1 \tag{16}$$

$$f_1(V) = 2\beta^4 V^3 e^{-\beta^2 V^2} \tag{17}$$

$$f_2(V) = \frac{4\beta^3}{\sqrt{\pi}} V^2 e^{-\beta^2 V^2} \tag{18}$$

$$\beta = \sqrt{\frac{AM}{2kT}} \tag{19}$$

$M_n$ is the mass of a neutron and $k$ is the Boltzmann constant.

To determine the velocity of the target, $V$ needs to be sampled from $f_1(V)$ with a probability of $P_1$, or from $f_2(V)$ with a probability of $P_2$. Secondly, the cosine of the angle between the neutron velocity and the target velocity is sampled uniformly on[−1,1]. Thirdly, this sampling is accepted with a probability of $\frac{v_r}{v_n+V}$.

### 2.2.3. *DBRC*

The DBRC method was designed to consider the thermal agitation and resonance of elastic scattering at the same time. The modified probability density function can be written as:

$$P(V,\mu|v_n) = C'\left\{\frac{\sigma_s(v_r,0)}{\sigma_s^{\max}(v_\xi,0)}\right\}\left\{\frac{v_r}{v_n+V}\right\}\{P_1 f_1(V) + P_2 f_2(V)\} \tag{20}$$

where

$$C' = \frac{(2+\sqrt{\pi}\beta v_n)\sigma_s^{\max}(v_\xi,0)}{2\sigma_s^{\mathrm{eff}}(v_n,T)\sqrt{\pi}\beta v_n} \tag{21}$$

$$v_\xi \in \left[v_n - \frac{4}{\sqrt{\alpha}}, v_n + \frac{4}{\sqrt{\alpha}}\right] \tag{22}$$

$$\alpha = \frac{M_t}{2kT} \tag{23}$$

$\sigma_s^{\max}(v_\xi,0)$ is the maximum value of the elastic scattering cross sections within a range of the dimensionless speed of $v_\xi$.

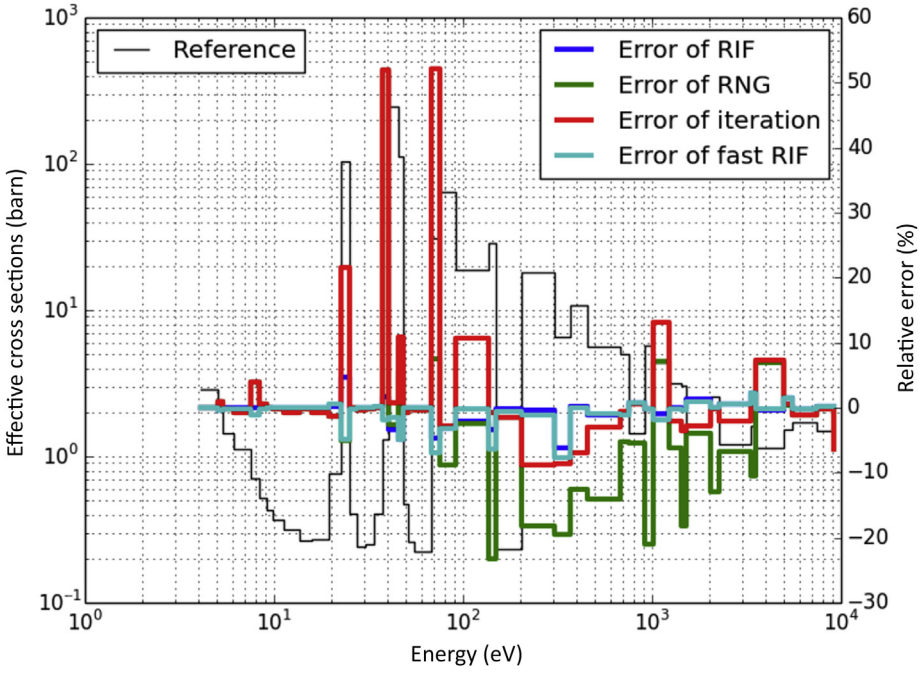


**Fig. 4 – Errors of effective absorption self-shielded cross section for $^{240}$Pu. RIF, resonance interference factor; RNG, resonant nuclide grouping.**

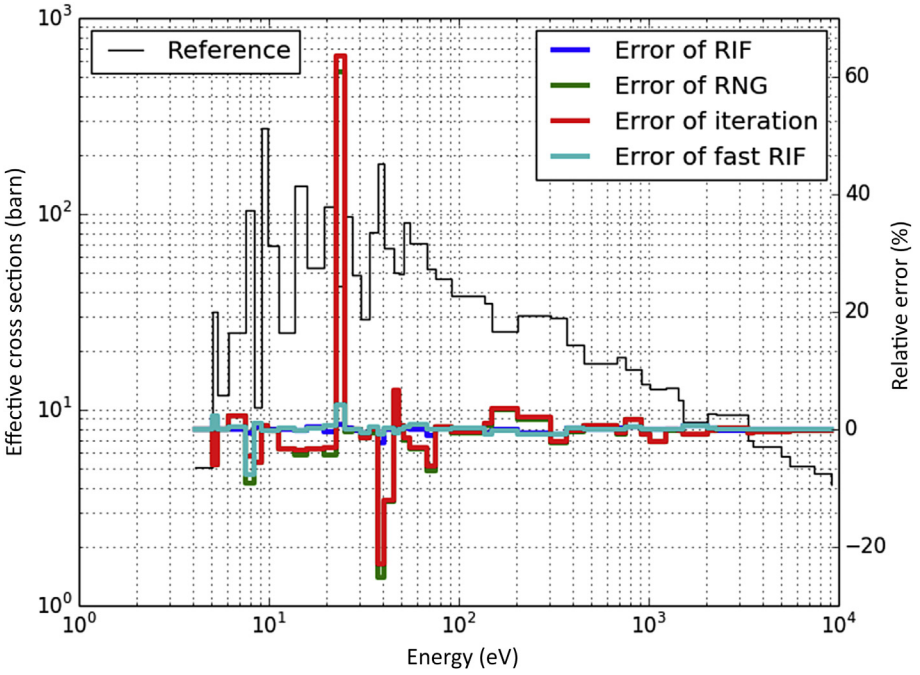


**Fig. 5 – Errors of effective absorption self-shielded cross section for $^{235}$U. RIF, resonance interference factor; RNG, resonant nuclide grouping.**

The difference between Eq. (20) and Eq. (13) is the additional rejection term in Eq. (20). During the sampling of the target velocity from Eq. (20), the accepting probability in the additional fourth step becomes $\sigma_s(v_r,0)/\sigma_s^{\max}(v_\xi,0)$.

### 2.2.4. *Resonance elastic scattering correction in subgroup method*

To consider the resonance elastic scattering effect in the subgroup method, self-shielded cross sections with and without the resonance elastic scattering effect, are calculated by OpenMC [20]. The resonance elastic scattering correction factor can be obtained by:

$$f_{g,k}(\sigma_b,T)=\frac{\sigma_{g,k}^{\mathrm{DBRC}}(\sigma_B,T)}{\sigma_{g,k}^{\mathrm{free}}(\sigma_B,T)} \tag{24}$$

These factors are prepared as a function of the background cross section and temperature in the multigroup library. An

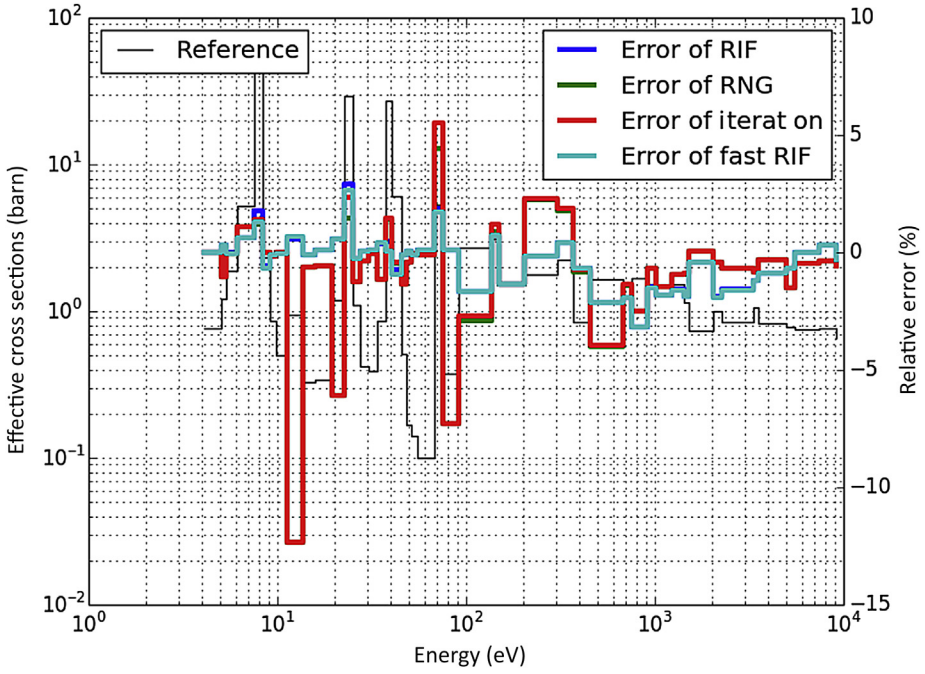


**Fig. 6 – Errors of effective absorption self-shielded cross section for $^{238}$U. RIF, resonance interference factor; RNG, resonant nuclide grouping.**

**Table 2 – Comparison of time for resonance calculation.**

| Method | SFSP (*n*) | SDP (*n*) | Time for resonance calculation (sec) |
|---|---|---|---|
| Iteration | 564 | 0 | 108.03 |
| RNG | 282 | 0 | 55.26 |
| RIF | 282 | 18 | 106.72 |
| Fast RIF | 47 | 3 | 23.69 |

RIF, resonance interference factor; RNG, resonant nuclide grouping; SDP, slowing down problem; sec, second; SFSP, subgroup fixed source problem.

interpolation can be done once the background cross section and temperature is ready. The factor can then be applied to correct the self-shielded cross sections.

### 2.3. *The resonance interference effect correction*

#### 2.3.1. *The Bondarenko iteration method*

Both the RI tables and the probability tables are obtained without considering the resonance interference effect. Practically, however, there are multiple resonant nuclides mixed together. The flux spectra interfere with each other, so that the self-shielded cross sections are different from those where only one resonant nuclide is considered as resonant. Correspondingly, most lattice codes adopt the Bondarenko iteration method [21].

The computation flow of the Bondarenko iteration method is as follows. Firstly, taking resonant nuclide $k$ as the only resonant nuclide, with all of the others as nonresonant nuclides. The macroscopic subgroup cross sections of the resonant region $m$ can be obtained by:

$$\sum_{x,m,g,i} = N_{k,m}\sigma_{x,k,g,i} + \sum_{k'\neq k} N_{k',m}\sigma_{x,k',g} \tag{25}$$

For nuclides without significant resonance, their microscopic cross sections, $\sigma_{x,k',g}$ can be directly read from the multigroup nuclear data library. For resonant nuclides assumed to be nonresonant, their microscopic cross sections can be updated iteratively by starting from a guess at the beginning. After the subgroup resonance calculation, the self-shielded cross section of nuclide $k$ can be obtained by Eq. (9). This process can then be repeated by setting another resonant nuclide as the only nuclide until all of the self-shielding cross sections are converged.

As the number of resonant nuclides may be large due to depletion, a resonant nuclide grouping (RNG) technique can be applied to reduce the computation time. Resonant nuclides are divided into categories according to their resonance features. In each resonance category, one representative nuclide is selected. During the Bondarenko iteration, one resonance category is treated as one resonant nuclide. The subgroup probabilities of one resonance category are assumed to be the same. Then the subgroup cross section can be calculated by:

$$\sigma_{c,m,x,g,i} = \frac{\sum_{k\in C_c} N_{k,m}\sigma_{x,k,g,i}}{\sum_{k\in C_c} N_{k,m}} \approx \frac{\sum_{k\in C_c} N_{k,m}\frac{R_{k,g,\infty}}{R_{r,g,\infty}}\sigma_{x,r,g,i}}{\sum_{k\in C_c} N_{k,m}} \tag{26}$$

where $c$ is the category index, $C_c$ is the nuclide indexes of category $c$, $r$ is the index of the representative nuclide, and $R_{k,g,\infty}$ is the resonance integral at infinite dilution cross section. The self-shielded cross sections of the representative nuclide are updated by the subgroup flux according to Eq. (9) and those of the nonrepresentative nuclides are updated by:

$$\sigma_{x,k,g} = \frac{R_{k,g,\infty}}{R_{r,g,\infty}}\sigma_{x,r,g} \tag{27}$$

In the lattice code HELIOS [41], the resonance categories are the same for different resonance energy groups. The code may not introduce much error when the number of energy groups is < 100, but when a finer energy group structure such as 172-group XMAS mesh is used, it is possible that in one energy group there is no resonance peak for the representative nuclide, but strong resonance peaks for the others. In this case, the errors of the self-shielded cross sections of the nonrepresentative nuclides may become very large. To overcome this defect, the resonance categories are determined to be different for different energy groups. A variable named resonance severity (*RS*) can be defined to characterize the intensity of the resonance.

$$RS_{k,m,g} = N_{k,m}R^{max}_{t,k,g} \Big/ R^{min}_{t,k,g} \tag{28}$$

where $R^{max}_{t,k,g}$ and $R^{min}_{t,k,g}$ are the maximum and minimum RI in the RI table, the quotient of which means the resonance intensity

**Table 3 – Comparison of the $k_\infty$ for mixed oxide pin cell problems.**

| Condition | $PuO_2$ content (wt.%) | Reference | Error (percent mille) | | | |
|---|---|---|---|---|---|---|
| | | | Iteration | RNG | RIF | Fast RIF |
| HFP | 1.0 | 0.93873 | −135 | −115 | −159 | −120 |
| | 2.0 | 1.01406 | −170 | −148 | −154 | −131 |
| | 4.0 | 1.06983 | −207 | −150 | −157 | −125 |
| | 6.0 | 1.09933 | −243 | −152 | −164 | −138 |
| | 8.0 | 1.12331 | −272 | −155 | −158 | −148 |
| HZP | 1.0 | 0.94671 | −140 | −130 | −131 | −102 |
| | 2.0 | 1.02307 | −159 | −142 | −113 | −93 |
| | 4.0 | 1.07949 | −196 | −132 | −128 | −107 |
| | 6.0 | 1.1089 | −213 | −114 | −123 | −106 |
| | 8.0 | 1.13299 | −249 | −123 | −130 | −128 |

HFP, hot full power; HZP, hot zero power; RIF, resonance interference factor; RNG, resonant nuclide grouping.

**Table 4 – Comparison of the $k_\infty$ for $UO_2$ pin cell problems.**

| Condition | Enrichment (%) | Reference | Error (percent mille) | | | |
|---|---|---|---|---|---|---|
| | | | Iteration | RNG | RIF | Fast RIF |
| HFP | 0.711 | 0.66435 | −110 | −110 | −138 | −103 |
| | 1.6 | 0.95649 | −133 | −133 | −152 | −143 |
| | 2.4 | 1.09335 | −137 | −137 | −140 | −113 |
| | 3.1 | 1.17098 | −158 | −158 | −152 | −126 |
| | 3.9 | 1.2334 | −171 | −171 | −150 | −127 |
| | 4.5 | 1.26872 | −176 | −176 | −144 | −123 |
| | 5.0 | 1.29312 | −188 | −188 | −148 | −127 |
| HZP | 0.711 | 0.66902 | −118 | −118 | −110 | −86 |
| | 1.6 | 0.96307 | −137 | −137 | −119 | −122 |
| | 2.4 | 1.10091 | −151 | −151 | −119 | −99 |
| | 3.1 | 1.1788 | −161 | −161 | −118 | −100 |
| | 3.9 | 1.24161 | −184 | −184 | −128 | −111 |
| | 4.5 | 1.27701 | −185 | −185 | −114 | −103 |
| | 5.0 | 1.30144 | −193 | −194 | −114 | −103 |

HFP, hot full power; HZP, hot zero power; RIF, resonance interference factor; RNG, resonant nuclide grouping.

in the microscopic scale, and $RS_{k,m,g}$ means the resonance intensity in the macroscopic scale. All of the resonant nuclides are sorted by resonance intensity in a decreasing order. For example, if $C$ categories are desired, the first $C-1$ resonant nuclides make the $C-1$ categories, while all of the remaining resonant nuclides make the last category, within which the resonant nuclide with the maximum resonance intensity is selected as the representative.

### 2.3.2. *Fast RIF method*

The calculation flow of the fast RIF method is as follows. (1) Select the dominant resonant nuclide of group $g$ according to the magnitude of $RS_{k,g}$ defined by Eq. (28). (2) Perform the resonance calculation for the dominant resonant nuclide in Group $g$, with all other resonant nuclides considered as background nuclides whose absorption cross section is zero and scattering cross section is equal to the potential scattering cross section. The self-shielded cross section of the dominant resonant nuclide is obtained by Eq. (9). (3) Convert the heterogeneous system to an equivalent homogeneous system for each resonant region $m$ by preserving the self-shielding cross section of the dominant resonant nuclide. The homogeneous system consists of all the resonant nuclides in resonant region $m$ and a pseudo nuclide whose atomic weight ratio is identical to that of $^1H$. The absorption cross section of the pseudo nuclide is zero and the macroscopic scattering cross section is given by:

$$\sum_{s,m,g,pseudo} = \sigma_{0,dom,m,g} N_{dom,m} - \sum_{k' \neq dom} \sigma_{p,k'} N_{k',m} \tag{29}$$

where $\sigma_{0,dom,m,g}$ is the equivalent microscopic dilution cross section in resonant region $m$, which is obtained by interpolation in the RI table of the dominant nuclide with the self-shielded cross section calculated in the second step. $N_{dom,m}$ is the number density of the dominant nuclide in resonant region $m$. The subscript $dom$ stands for the dominant resonant nuclide. $\sum_{k' \neq dom} \sigma_{p,k'} N_{k',m}$ is the macroscopic potential scattering cross section of the resonant nuclides other than the dominant resonant nuclide. (4) The above three steps are carried out for each resonance energy group. Therefore, for each resonant region, an equivalent homogeneous system can be found. The homogeneous system consists of a mixture of resonant nuclides and a pseudo nuclide, whose macroscopic scattering cross sections vary with the energy group. The number density of the pseudo nuclide is set to be $N_{m,pseudo}$ and the microscopic scattering cross section of each energy group is obtained by:

$$\sigma_{s,m,g,pseudo} = \frac{\Sigma_{s,m,g,pseudo}}{N_{m,pseudo}} \tag{30}$$

The slowing down problem of the constructed homogeneous system is solved with the hyperfine energy group method. The obtained self-shielding cross sections of the resonant nuclides in the mixture are the effective self-shielded cross sections considering the resonance interference effect.

To compare the precision and efficiency between the conventional and the fast RIF methods, a kind of conventional RIF method is also implemented in this paper. The conventional RIF method carries out the above steps, from Step 2 to Step 4, for each resonant nuclide. When one resonant nuclide is under consideration, it is treated as the dominant nuclide. In Step 4, only the self-shielded cross sections of the resonant nuclide under consideration are updated.

**Table 5 – Composition of the fuel of the depletion case.**

| Nuclide | Density |
|---|---|
| $^{16}O$ | 4.6019200E-02 |
| $^{99}Tc$ | 7.7111100E-05 |
| $^{235}U$ | 1.5673502E-04 |
| $^{238}U$ | 2.0719173E-02 |
| $^{237}Np$ | 2.6500062E-05 |
| $^{238}Pu$ | 1.6212906E-05 |
| $^{239}Pu$ | 1.6925900E-04 |
| $^{240}Pu$ | 7.8198341E-05 |
| $^{241}Pu$ | 5.1843213E-05 |
| $^{242}Pu$ | 2.4885304E-05 |
| $^{241}Am$ | 2.1594599E-06 |
| $^{243}Am$ | 8.8360858E-06 |

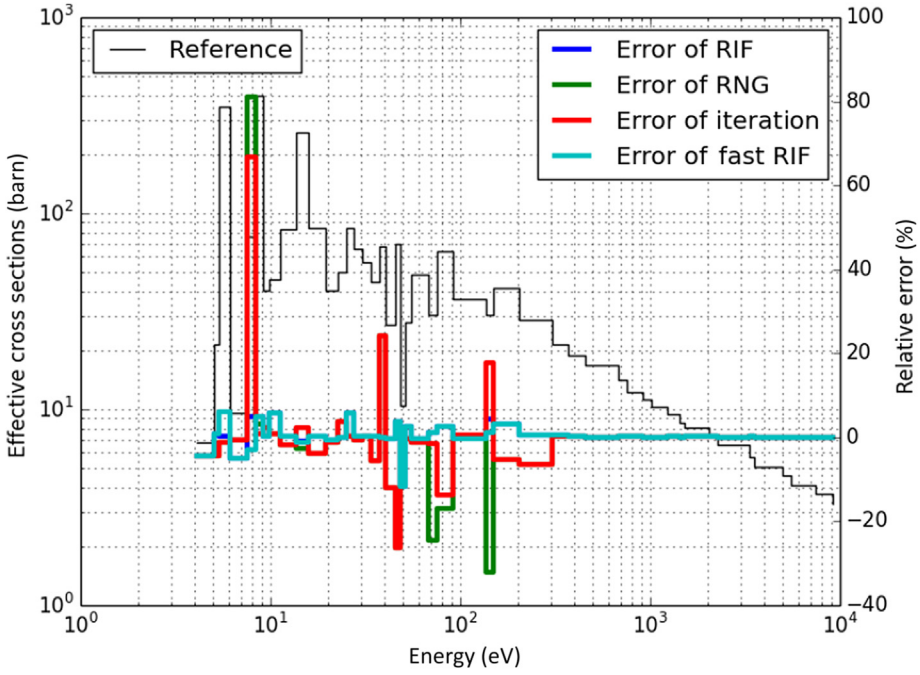


**Fig. 7 – Errors of effective absorption self-shielded cross section for $^{243}$Am in the depletion case. RIF, resonance interference factor; RNG, resonant nuclide grouping.**

## 3. Numerical results

Based on the DBRC method, the OpenMC code has been modified. The new sampling scheme is applied to cases where $A_k$ is > 50 and neutron energy locates in the range of 0.4–210 eV. The RI tables and the resonance elastic scattering correction factor tables of $^{235}$U, $^{238}$U, $^{239}$Pu, $^{240}$Pu, $^{241}$Pu, and $^{242}$Pu are prepared by OpenMC. The RI tables of other resonant nuclides are prepared by RMET21 [38] to save computational time. The probability tables are prepared based on the RI tables without consideration of the resonance elastic scattering effect. The other part of the multigroup library is generated by NJOY. The library is based on ENDF/B-VII.0. The multigroup library is generated based on the 172-group XMAS mesh [42],

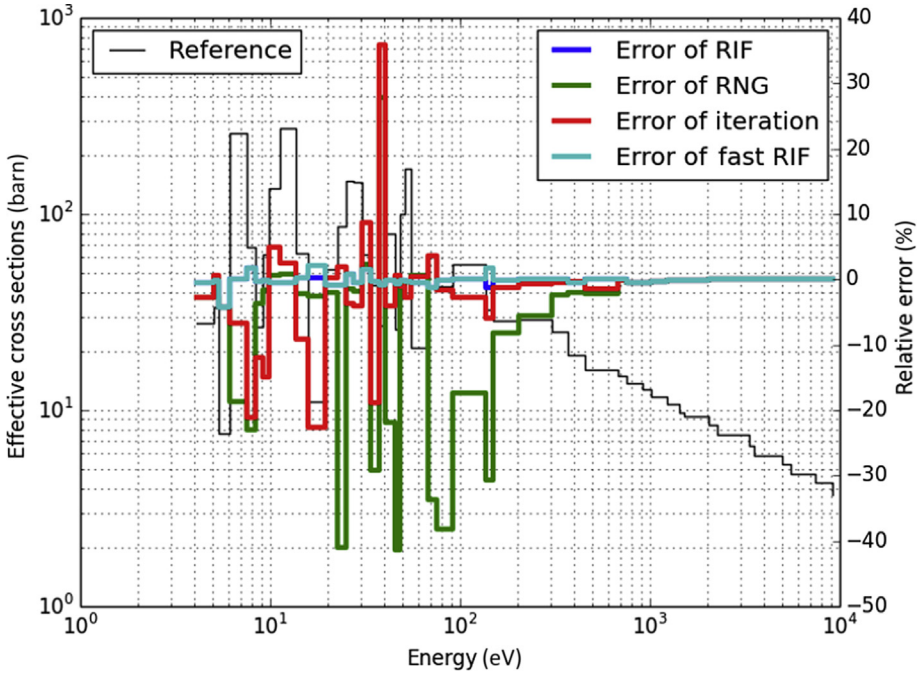


**Fig. 8 – Errors of effective absorption self-shielded cross section for $^{237}$Np in the depletion case. RIF, resonance interference factor; RNG, resonant nuclide grouping.**

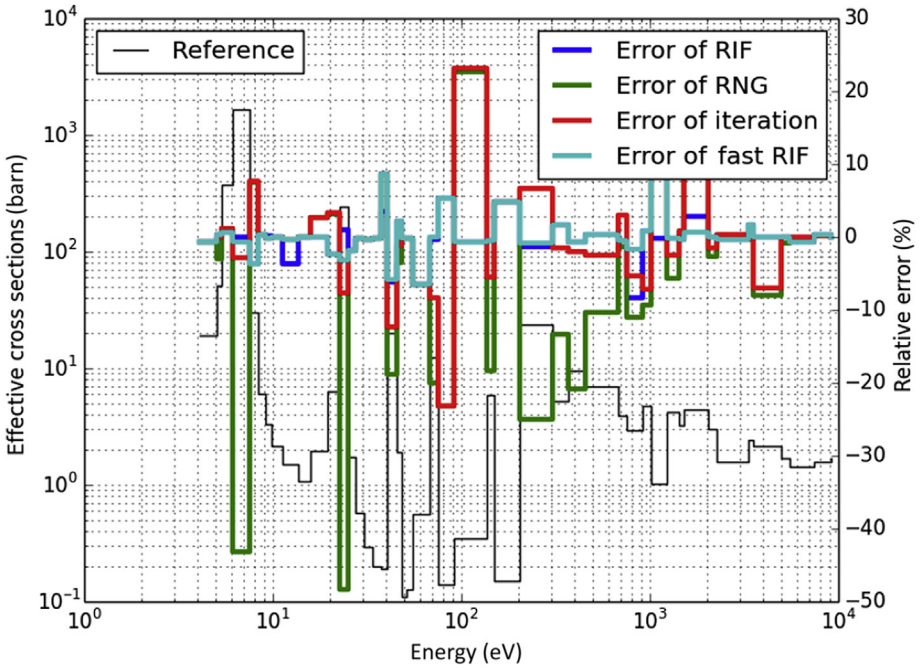


**Fig. 9 – Errors of effective absorption self-shielded cross section for $^{99}$Tc in the depletion case. RIF, resonance interference factor; RNG, resonant nuclide grouping.**

and the self-shielding is treated in the energy range of 4.0–9,119 eV from Group 46 to Group 92. The resonance elastic scattering correction method, Bondarenko iteration method, conventional RIF method and fast RIF method are implemented into a subgroup method code: SUGAR [43,44].

### 3.1. *The resonance elastic scattering effect correction*

The Mosteller Doppler defect benchmark [45] is analyzed by using both SUGAR and the modified OpenMC. The difference of eigenvalues for the $UO_2$ pin cell problems at hot zero power (HZP) and hot full power (HFP) between the conventional scattering kernel and the Doppler broadened scattering kernel are given in Figs. 2 and 3. For comparison, references are provided including MVP-WCM (MVP [18] with WCM and the Doppler broadened scattering kernel), MCNP6-DBRC (MCNP6 [46] with DBRC), TRIPOLI-DBRC and TRIPOLI-WCM (TRIPOLI [10] with DBRC and WCM respectively). It can be found that SUGAR provides consistent results with the others. For the $UO_2$ pin cell, the asymptotic scattering kernel overestimates the eigenvalues by 30–140 percent mille (pcm) at HZP and 80–230 pcm at HFP.

### 3.2. *The resonance interference effect correction*

The resonance severity (*RS*) of different nuclides are given in Table 1 for the Mosteller benchmark MOX pin cell problem at HZP with 8% $PuO_2$. As the values of *RS* vary with each energy group, only *RS* for the 80$^{th}$ energy group are given. For this group, $^{238}$U is selected as the dominant resonant nuclide in the fast RIF method. In the RNG method, if the number of categories is three, $^{238}$U and $^{239}$Pu make the first two categories while $^{240}$Pu, $^{241}$Pu, $^{235}$U, and $^{242}$Pu make the third group with $^{240}$Pu being the typical nuclide.

The Mosteller benchmark problems are analyzed by using different resonance interference methods without resonance elastic scattering correction. The reference self-shielded cross sections are estimated by OpenMC with the conventional free gas model. To get rid of the data library or data processing errors, the reference $k_\infty$ is calculated using the reference self-shielded cross sections and other cross sections read from the multigroup nuclear library by using the transport solver of SUGAR.

The errors of the effective absorption cross sections for the MOX pin cell problem at HZP are provided in Figs. 4–6. The $PuO_2$ content in the fuel is 8%. It is shown that the errors of the Bondarenko iteration method and the RNG method are larger than those of the RIF method and the fast RIF method, especially for $^{240}$Pu (as in Fig. 4) and $^{235}$U (as in Fig. 5). The resonance of those two nuclides is weak, but they are fiercely interfered with by the dominant resonant nuclide $^{238}$U (as in Fig. 6). The error of the iteration method and the RNG method belongs to the same level for the representative resonant nuclides $^{235}$U (as in Fig. 5) and $^{238}$U (as in Fig. 6). For the nonrepresentative $^{240}$Pu (as in Fig. 4), the errors of these two methods differentiate from each other significantly. By

**Table 6 – Comparison of $k_\infty$ for mixed oxide pin cell problems at hot zero power.**

| $PuO_2$ content (%) | Reference | Error (percent mille) | | |
|---|---|---|---|---|
| | | Scheme 1 | Scheme 2 | Scheme 3 |
| 1.0 | 0.94640 | −79 | −172 | −150 |
| 2.0 | 1.02211 | −107 | −198 | −161 |
| 4.0 | 1.07766 | −148 | −234 | −179 |
| 6.0 | 1.10599 | −181 | −262 | −189 |
| 8.0 | 1.12951 | −200 | −276 | −189 |

contrast, both the fast and the conventional RIF methods are in good agreement with the reference.

The times taken for the resonance calculation, including the time for the subgroup fixed source calculation and the slowing down calculation, is compared in Table 2. Compared with the Bondarenko iteration method, the RNG method groups the six resonant nuclides into three categories and saves half of the time. Compared with the conventional RIF method, only one resonant nuclide is chosen to perform a subgroup fixed source calculation in the fast RIF method, and the slowing down calculations are carried out once for all the nuclides rather than for each nuclide. The speedup of the fast RIF method is ~4.56. In general, the Bondarenko iteration method and the conventional RIF method consume the longest times, and the fast RIF method consumes the least.

The errors of $k_\infty$ for the MOX and $UO_2$ pin cell problems are compared in Tables 3 and 4 respectively. For most cases, the RIF and the fast RIF method gain higher precision than the Bondarenko iteration method. The precisions of the RIF and the fast RIF methods are at the same level. For the $UO_2$ pin cell problems, there are only two resonant nuclides so that there is no typical resonant nuclide in the RNG method. Therefore, the RNG method and the Bondarenko iteration method are of no difference. For the MOX pin cell problems, the errors of the RNG method tend to be cancelled out due to the overestimation of $^{238}U$ absorption and the underestimation of the absorption of plutonium nuclides.

The geometry of the depletion case is the same as that of the Mosteller benchmark $UO_2$ problem at HFP condition. The nuclide densities in the fuel region are given in Table 5. The self-shielded cross sections of $^{243}Am$, $^{237}Np$ and $^{99}Tc$, calculated by different resonance interference correction methods, are compared in Figs. 7–9. The conventional RIF method and the fast RIF method shows advantages over the Bondarenko iteration method and the RNG method.

### 3.3. *The combined resonance elastic scattering and interference effects corrections*

Table 6 compares the $k_\infty$ for the MOX pin cell problems at HZP with different correction schemes. The references are calculated by OpenMC with the DBRC method. Scheme 1 applies the Bondarenko iteration without resonance elastic scattering correction. Scheme 2 applies the Bondarenko iteration and resonance elastic scattering correction. Scheme 3 applies fast RIF and resonance elastic scattering correction. The resonance elastic scattering correction makes a negative contribution to the $k_\infty$ since more neutrons are absorbed due to upscattering. On the contrary, the fast RIF resonance interference correction makes a positive contribution. Therefore the errors may be cancelled out when neither of these two effects is considered. When the $PuO_2$ content is low, the resonance interference is not that fierce and the advantage of fast RIF over the Bondarenko iteration is not obvious. Therefore the results of Scheme 1 are better than those of Scheme 3 in terms of $k_\infty$. When the $PuO_2$ content is high, the advantage of fast RIF is obvious, so that the correction of resonance interference overwhelms the correction of resonance elastic scattering.

## 4. Conclusions

Two aspects of the legacy subgroup method were improved upon. Firstly, the resonance elastic scattering effect is considered. The Mosteller benchmark problems were analyzed. The numerical results show that the Doppler broadened scattering kernel decreases $k_\infty$ 30–140 pcm at HZP and 80–230 pcm in HFP for light-water reactor $UO_2$ pin cell problems.

Secondly, the fast RIF method is proposed to improve the computational efficiency of the resonance interference effect treatment. Four methods are compared and analyzed, including the conventional Bondarenko iteration method, the RIF method, and the new fast RIF method. The numerical results lead to encouraging conclusions. Compared with the RIF method, the fast RIF method provides effective self-shielded cross sections with equivalent accuracy which is an improvement on the Bondarenko iteration method. For computing efficiency, compared to the iteration method, the RNG method saves half of the computation time for the MOX pin cell problems, while the fast RIF method consumes much less computational resources. The speedup of the fast RIF method is ~4.56 for MOX pin cell problems compared the conventional RIF method.

## Conflicts of interest

All authors have no conflicts of interest to declare.

## Acknowledgments

This work was financially supported by the National Natural Science Foundation of China (No. 11305123) and Science and Technology on Reactor System Design Technology Laboratory.

## REFERENCES

[1] A. Hébert, The Ribon extended self-shielding model, Nucl. Sci. Eng. 151 (2005) 1–24.
[2] T. Takeda, H. Fujimoto, K. Sengoku, Application of multiband method to KUCA tight-pitch lattice analysis, J. Nucl. Sci. Technol. 28 (1991) 863–869.
[3] H.G. Joo, J.Y. Cho, K.S. Kim, C.C. Lee, S.Q. Zee, Methods and performance of a three-dimensional whole-core transport code DeCART, in: Proceedings of the Physics of Fuel Cycles and Advanced Nuclear Systems: Global Developments (PHYSOR) 2004, Chicago (IL), April 25–29, 2004.
[4] Y.S. Jung, C.B. Shim, C.H. Lim, H.G. Joo, Practical numerical reactor employing direct whole core neutron transport and subchannel thermal/hydraulic solvers, Ann. Nucl. Energy 62 (2013) 357–374.
[5] Y. Liu, B. Collins, B. Kochunas, W. Martin, K. Kim, M. Williams, Resonance self-shielding methodology in mpact, in: Proceedings of Mathematics and Computational Methods Applied to Nuclear Science & Engineering (M&C) 2013, Sun Valley (ID), May 5–9, 2013.
[6] H.G. Joo, G.Y. Kim, L. Pogosbekyan, Subgroup weight generation based on shielded pin-cell cross section conservation, Ann. Nucl. Energy 36 (2009) 859–868.
[7] R.E. MacFarlane, NJOY99.0: a Code System for Producing Pointwise and Multigroup Neutron and Photon Cross

Sections from ENDF/B Evaluated Nuclear Data, 2000. Los Alamos (NM).
[8] X-5 Monte Carlo Team, MCNP—a General Monte Carlo n-particle Transport Code, Version 5, 2003. Los Alamos, New Mexico.
[9] D. Lee, K. Smith, J. Rhodes, The impact of $^{238}$U resonance elastic scattering approximations on thermal reactor Doppler reactivity, in: Proceedings of International Conference on the Physics of Reactors (PHYSOR) 2008, Interlaken (Switzerland), September 14–19, 2008.
[10] A. Zoia, E. Brun, C. Jouanne, F. Malvagi, Doppler broadening of neutron elastic scattering kernel in Tripoli-4, Ann. Nucl. Energy 54 (2013) 218–226.
[11] B. Becker, On the Influence of the Resonance Scattering Treatment in Monte Carlo Codes on High Temperature Reactor Characteristics, University of Stuttgart, Stuttgart (Germany), 2010.
[12] C.H. Lim, Y.S. Jung, H.G. Joo, Incorporation of resonance upscattering and intra-pellet power profile in direct whole core calculation, in: Conf. Korean Nucl. Soc, 2012.
[13] L. Mao, I. Zmijarevic, The Up-scattering Treatment in the Fine-structure Self-shielding Method in APOLLO3, in: Proceedings of International Conference on the Physics of Reactors (PHYSOR) 2014, The Westin Miyako, Kyoto, Japan, September 28 – October 3, 2014.
[14] M. Ouisloumen, R. Sanchez, A model for neutron scattering off heavy isotopes that accounts for thermal agitation effects, Nucl. Sci. Eng. 107 (1991) 189–200.
[15] W. Rothenstein, Proof of the formula for the ideal gas scattering kernel for nuclides with strongly energy dependent scattering cross sections, Ann. Nucl. Energy 31 (2004) 9–23.
[16] R. Dagan, On the use of S(α,β) tables for nuclides with well pronounced resonances, Ann. Nucl. Energy 32 (2005) 367–377.
[17] B. Becker, R. Dagan, G. Lohnert, Proof and implementation of the stochastic formula for ideal gas, energy dependent scattering kernel, Ann. Nucl. Energy 36 (2009) 470–474.
[18] T. Mori, Y. Nagaya, Comparison of resonance elastic scattering models newly implemented in MVP continuous-energy Monte Carlo code, J. Nucl. Sci. Technol. 46 (2009) 793–798.
[19] H.J. Shim, B.S. Han, J.S. Jung, H.J. Park, C.H. Kim, Mccard: Monte Carlo code for advanced reactor design and analysis, Nucl. Eng. Technol. 44 (2012) 161–176.
[20] P.K. Romano, B. Forget, The OpenMC Monte Carlo particle transport code, Ann. Nucl. Energy 51 (2013) 274–281.
[21] J.R. Askew, F.J. Fayers, P.B. Kemshell, A general description of lattice code WIMS, J. Br. Nucl. Energy Soc. 5 (1966) 546–585.
[22] T. Takeda, Y. Kanayama, A multiband method with resonance interference effect, Nucl. Sci. Eng. 131 (1999) 401–410.
[23] S.E. Huang, K. Wang, D. Yao, An advanced approach to calculation of neutron resonance self-shielding, Nucl. Eng. Des. 241 (2011) 3051–3057.
[24] A. Hébert, A mutual resonance shielding model consistent with Ribon subgroup equations, in: PHYSOR 2004, Chicago (IL), April 25–29, 2004.
[25] M.L. Williams, Correction of multigroup cross sections for resolved resonance interference in mixed absorbers, Nucl. Sci. Eng. 83 (1993) 37–49.
[26] G. Chiba, A combined method to evaluate the resonance self shielding effect in power fast reactor fuel assembly calculation, J. Nucl. Sci. Technol. 40 (2003) 537–543.
[27] K. Kim, M.L. Williams, Preliminary assessment of resonance interference consideration by using 0-D slowing down calculation in the embedded self-shielding method, Trans. Am. Nucl. Soc. 109 (2012).
[28] K.S. Kim, S.G. Hong, A new procedure to generate resonance integral table with an explicit resonance interference for transport lattice codes, Ann. Nucl. Energy 38 (2011) 118–127.
[29] S. Peng, X. Jiang, S. Zhang, D. Wang, Subgroup method with resonance interference factor table, Ann. Nucl. Energy 59 (2013) 176–187.
[30] D.J. Powney, T.D. Newton, Overview of the WIMS 9 Resonance Treatment, Serco Assurance, Dorchester, 2004.
[31] E. Wehlage, D. Knott, V.W. Mills, Modeling resonance interference effects in the lattice physics code LANCER02, in: Proceedings of Mathematics and Computational Methods Applied to Nuclear Science & Engineering (M&C) 2005, Avignon (France), September 12–15, 2005.
[32] Y. Liu, W. Martin, M. Williams, K.S. Kim, A full-core resonance self-shielding method using a continuous-energy quasi–one-dimensional slowing-down solution that accounts for temperature-dependent fuel subregions and resonance, Nucl. Sci. Eng. 180 (2015) 247–272.
[33] Y. Liu, W.R. Martin, K.S. Kim, M.L. Williams, Modeling resonance interference by 0-D slowing-down solution with embedded self-shielding method, in: Proceedings of Mathematics and Computational Methods Applied to Nuclear Science & Engineering (M&C) 2013, Sun Valley (ID), May 5–9, 2013.
[34] S. Choi, A. Khassenov, D. Lee, Resonance self-shielding method using resonance interference factor library for practical lattice physics computations of LWRs, J. Nucl. Sci. Technol. (2015). Available from: http://dx.doi.org/10.1080/00223131.2015.1095686.
[35] L. Mao, R. Sanchez, I. Zmijarevic, Considering the up-scattering in resonance interference treatment in APOLLO3, in: Proceedings of Mathematics and Computational Methods Applied to Nuclear Science & Engineering (M&C) 2015, Nashville (TN), April 19–23, 2015.
[36] A. Hébert, Applied Reactor Physics, Presses Inter Polytechnique, 2009.
[37] H. Zhang, H. Wu, L. Cao, An acceleration technique for 2D MOC based on Krylov subspace and domain decomposition methods, Ann. Nucl. Energy 38 (2011) 2742–2751.
[38] F. Leszczynski, Neutron resonance treatment with details in space and energy for pin cells and rod clusters, Ann. Nucl. Energy 14 (1987) 589–601.
[39] Y. Ishiguro, H. Takano, PEACO: a Code for Calculation of Group Constant of Resonance Energy Region in Heterogeneous Systems, JAERI, 1971.
[40] P.H. Kier, A.A. Robba, Rabble, a Program for Computation of Resonance Absorption in Multiregion Reactor Cells, 1967.
[41] R.J.J. Stamm'ler, HELIOS Methods, Studsvik Scandpower, Waltham, 2001.
[42] E. Sartori, Standard Energy Group Structures of Cross Section Libraries for Reactor Shielding, Reactor Cell and Fusion Neutronics Applications: VITAMIN-J, ECCO-33, ECCO-2000 and XMAS, JEF/DOC-315, Revision 3, NEA Data Bank, Gif-sur-Yvette Cedex, France, 1990.
[43] L. He, H. Wu, L. Cao, Y. Li, Improvements of the subgroup resonance calculation code SUGAR, Ann. Nucl. Energy 66 (2014) 5–12.
[44] L. Cao, H. Wu, Q. Liu, Q. Chen, Arbitrary geometry resonance calculation using subgroup method and method of characteristics, in: Proceedings of Mathematics and Computational Methods Ap plied to Nuclear Science & Engineering (M&C) 2011, Rio de Janeiro (Brazil), May 8–12, 2011.
[45] R.D. Mosteller, Computational Benchmarks for the Doppler Reactivity Defect, Joint Benchmark Committee of the Mathematics and Computation, Radiation Protection and Shielding, and Reactor Physics Divisions of the American Nuclear Society, 2006.
[46] E.E. Sunny, F.B. Brown, B.C. Kiedrowski, W.R. Martin, Temperature effects of resonance scattering for epithermal neutrons in MCNP, in: PHYSOR 2012, April 15–20, 2012. Knoxville (TN).